World Academy of Science, Engineering and Technology
International Journal of Civil and Environmental Engineering
Vol:16, No:9, 2022

Creating 3D Models Using Infrared Thermography with Remotely Piloted Aerial Systems

P. van Tonder, C. C. Kruger

***Abstract*—**Concrete structures deteriorate over time and degradation escalates due to various factors. The rate of deterioration can be complex and unpredictable in nature. Such deteriorations may be located beneath the surface of the concrete at high elevations. This emphasizes the need for an efficient method of finding such defects to be able to assess the severity thereof. Current methods using thermography to find defects require equipment to reach higher elevations. This could become costly and time consuming not to mention the risks involved in having personnel scaffold or abseiling at such heights. Accordingly, by combining the thermal camera needed for thermography and a remotely piloted aerial system (Drone/RPAS), it could be used to alleviate some of the issues mentioned. Images can be translated into a 3D temperature model to aid concrete diagnostics and with further research can relate back to the mechanical properties of the structure but will not be dealt with in this paper. Such diagnostics includes finding delamination, similar to finding delamination on concrete decks, which resides beneath the surface of the concrete before spalling can occur. Delamination can be caused by reinforcement eroding and causing expansion beneath the concrete surface. This could lead to spalling, where concrete pieces start breaking off from the main concrete structure.

***Keywords*—**Concrete, diagnostic, infrared thermography, 3D thermal models.

I. Introduction

CONCRETE is a versatile and durable material however, it can be susceptible to deterioration. The deterioration of concrete may be due to multiple factors throughout the concrete's lifetime. Factors such as poor workmanship could lead to honeycombing, wrongly mixed proportions of the constituents or badly weathered reinforcement being used. The environment in which the concrete is in could also affect the acceleration of carbonation, leading to the corrosion of the steel reinforcement. Spalling and cracks could form and might be seen as a structural deterioration if it is severe [2]. Quality control is important in ensuring the concrete is produced, casted and maintained correctly. This process is important to ensure the desired lifespan of the concrete is achieved while maintaining its structural and visual needs. The need for testing and measuring whether the concrete is maintaining its needs is a crucial step in the process. Such tests, where concrete is already cast and set, include non-destructive testing. Such tests include visual inspection that are done by experienced professionals who can appropriately assess the severity and the next steps to take [2]. Doing such visual inspections can be a difficult and time-consuming activity especially on high-rise concrete structures. Ideally such a testing method should be done efficiently and effectively. One such non-destructive testing method could be by remote visual inspection, with a combination of infrared thermography. Infrared thermography is a non-destructive diagnostics method being used in various engineering fields. Its use in civil engineering is quite new and is limited by the lack of experience and the challenges involved with large structures and the need to be artificially heated, if passive heating from the sun is not sufficient. However, in Southern Africa such structures can be heated passively due to an abundance of sunshine [3].

Thermography captures and measures infrared radiation emitted by the object being measured. The amount of radiation emitted depends on the emissivity of an object. Emissivity is a dimensionless ratio of the radiation emitted from an object to that of a perfect blackbody both at the same temperature and wavelength measured [4]. The emissivity depends on the type of material, surface finishes, geometry, wavelength absorbed and reflected, viewing angle and the temperature [5]. Tests performed by van der Merwe have shown that acute viewing angles captured less radiation than that of a perpendicular viewing angle, providing no external reflections were captured [4]. Thermography being used as a tool to find points of interest on structures, like defects, has been used in previous construction projects. These projects, that received award of merit by International Concrete Repair Institute (ICRI) [11], included using thermography to find defects by means of large image scans and thermal images to find developing spalls [6]. The second is used to detect reinforced grouted cells and document where such cells are needed or needs repairs [6]. Thermography can also be used in other maintenance services such as characterization of tracks [7]. Remotely Piloted Aerial Systems (RPAS) have been part of various disciplines. Together with a thermal camera, the use for an RPAS can extend further from finding disaster survivors to finding hotspots on solar farms. This technology is widely used to monitor railway, roads and other infrastructure like inspecting high-voltage electricity pylon supports or wind turbines [8], [9]. The legislation regarding RPAS is still being fully developed. The Civil Aviation Authority (CAA) introduced new bylaws to accommodate RPAS into non-segregated airspace. The bylaws can be found in the Civil Aviation Act, 2009 (Act no. 13 of 2009) and state that a RPAS for commercial/corporate use must be approved by the director and the associated fees to be paid as stated in Part 187 [10]. The operator of the RPAS must

P. van Tonder is with the University of Johannesburg, Auckland Park, Johannesburg, 2000 (corresponding author, phone: +27115593250; e-mail: pierrevt@uj.ac.za).

C.C. Kruger was with the University of Johannesburg, Auckland Park, Johannesburg, 2000 (e-mail: christoffkruger2@gmail.com)

possess a license appropriate to the usage and class of the RPAS and should meet the requirements as per section 101.03.02. An additional air service license should also be issued for any commercial operations [10]. The use of a RPAS for private operations (where there is no commercial outcome/interest) is limited to Class 1A or 1B, where the RPAS weighs no more than 7 kg, may not be flown out of sight and may not be flown higher than 150 ft.

II. Background

A. Electromagnetic Waves

Visible light, X-rays, radio waves and also infrared are all characterized as being similar to how waves behave. These particular types of electromagnetic waves (EM), propagate through space with the speed of light c, being roughly 3 x 10^8 m/s in a vacuum (this speed is lower though matter as the speed through the matter depends on the refraction index n, thus the speed can be written as v = c/n) [12]. The wavelength (λ) is described by (1) (f-frequency; c-speed of light). See Fig. 1 for a schematic explanation, the mark moves up or down on the same horizontal position as the wave propagates forward. The time it takes for the red mark to move to its original position is described as the time for one oscillation. The inverse of this will be the frequency for that particular wavelength.

$$\lambda = \frac{c}{f} \tag{1}$$

The wavelength of the wave characterizes the wave according to the electromagnetic spectrum. The longest wavelength to shortest wavelength in order is as follows: radio waves, microwaves, infrared radiation, visible light, ultraviolet radiation, X-rays and gamma rays. Thus, infrared radiation has a wavelength smaller than microwaves (< 1 mm) and larger than visible light (> 0.78 μm). However, within that range of infrared radiation, IRT only makes use of shortwave (SW, ~ 0.8-1.7 μm), mediumwave (MW, ~ 3-5 μm) and longwave (LW, ~ 7-14 μm), see Fig. 2. The IR camera used for the tests uses long-wavelength (8-14 μm) infrared waves.

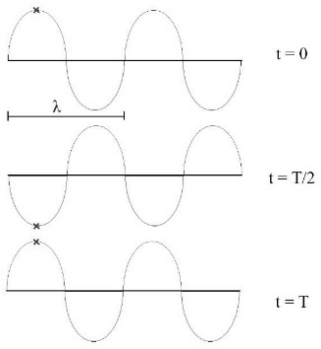

Fig. 1 Propagation of a sinusoidal wave

EM radiation occurs naturally, with the most important phenomena thereof called thermal radiation is what thermography is based on. Thermal radiation is roughly defined as a body having a temperature more than -273.15 °C (0 K) and will emit EM radiation. The radiation is wavelength dependent and the amount of radiation depends on the properties of the material and temperature. Natural temperatures and temperatures found in technological processes are in such a range that the radiation falls in the IR spectral region, thus applicable for thermography.

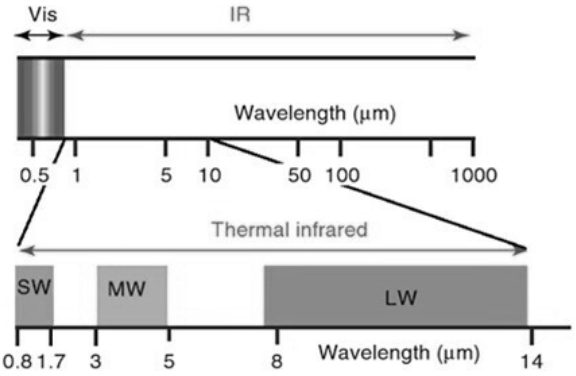

Fig. 2 Infrared wavelength used in thermal imaging (SW, MW & LW) [7]

B. Emissivity

Emissivity is defined as the radiant flux which an object emits to that of the radiant flux a blackbody emits, both at the same temperature. Planck's law defines the radiation released by a blackbody, but there are few surfaces which act according to this law and emit radiation less than what is predicted from their kinetic temperature. A blackbody emits all radiation absorbed and so Kirchoff's law states, the emittance is equal to the absorbance at a given temperature for a given wavelength. Accounting for the conservation of energy the sum of the reflection, absorption and transmission should equal 1, see (2) [13]. For opaque bodies, it would not transmit radiation and so the sum of absorption and reflection should equal 1, see (3) [13]. The emissivity is dependent on the surface type (features include; geometry, texture, type of material) and the wavelength [13]. Emissivity needs to be corrected as it could show false temperatures of a surface. For example, a polished metal will have a low emissivity (0.05) and accordingly it would radiate less than a rougher, non-metal which would have a higher emissivity (0.98). Thus, the metal would appear to be colder than the non-metal surface as shown in Fig. 3 [13].

$$\varepsilon_\lambda + \rho_\lambda + \tau_\lambda = 1 \tag{2}$$

$$\varepsilon_\lambda + \tau_\lambda = 1 \tag{3}$$

C. Viewing Angle

Emissivity can also vary by viewing angles. Observations orthogonally to the surface will show the true temperature (if emissivity of the surface is corrected for the thermal camera) whereas in observations done oblique to the surface, cooler apparent temperatures will be observed. This is due to surfaces being viewed at an angle will have lower emissivity. This can be seen in Fig. 4 where the cubes are made from the same

material but only the viewing angle to the surfaces is different, as a result a cooler top surface is observed. This is described schematically in Fig. 5 where an arbitrary object with emissivity of 0.95, at an orthogonal viewing angle, is viewed at decreasing angles. The emissivity slowly decreases and as the viewing angle passes 60° the emissivity rapidly decreases to a low emissivity of ~0.3 [12]. For the purpose of the project where mostly non-metal materials will be considered (concrete walls, silos), the emissivity is quite close to 1.0 (0.94 for concrete [14]). For such materials, when the viewing angle becomes more oblique (as viewing direction becomes parallel to surface area), more than 45°-60° from an orthogonal view would result in the emissivity decreasing drastically [4]. Thus, if the viewing angle is kept as orthogonal as possible, a constant emissivity can be used provided the surface is homogenous (which is mostly the case for concrete finishes).

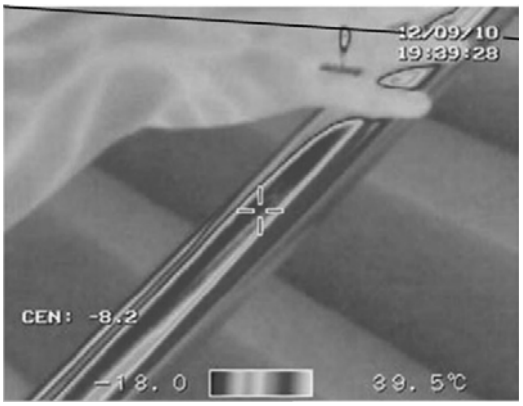

Fig. 3 Uncorrected emissivity at ambient temperature 22 °C of metal rail [13]

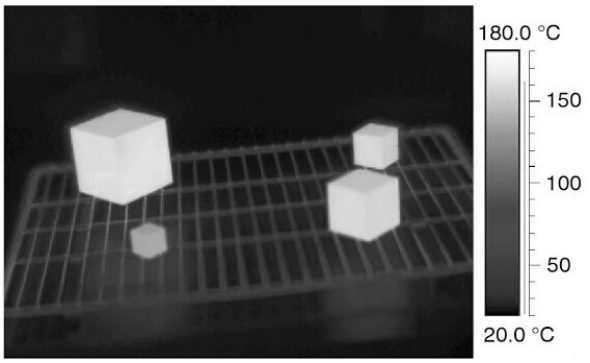

Fig. 4 Surface temperature of cubes at different angles [13]

D.Surface Finish

Emissivity is different depending on the finish of the surface being observed. This is evident when using a Leslie cube as shown in Fig. 6. A Leslie cube is a hollow copper cube with its faces finished differently: rough copper face, polished copper face, white painted face and the black painted face. The cube is placed on an insulator to ensure no thermal reflection is present. The cube is filled with warm water and observed in such a manner where each surface is observed from the same angle. Fig. 6 shows a cube with the Top-Left face (Polished copper) to be cooler than the adjacent sides. This is due to the low emissivity of polished copper. The top-right face being the white paint and the bottom face the black paint, both seem to be at roughly the same apparent temperature and might be due to the roughness of the paint surface, similar surface irregularities. Fig. 6 also shows a cube with the top-left face being the rough copper, this face appears to be slightly warmer than the top-right face (polished copper) but cooler than the black paint. Again, this is due to the roughness of the surface which causes diffuse scattering resulting in a slightly higher emissivity than that of the polished copper.

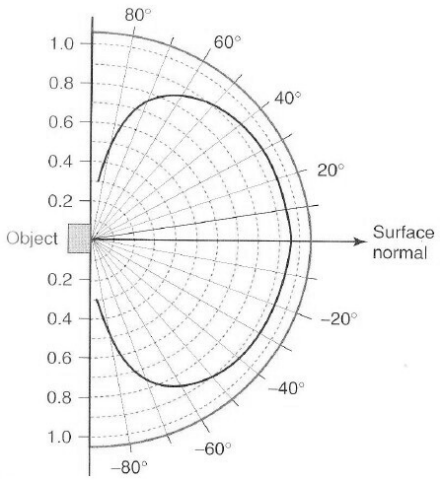

Fig. 5 Emissivity of a non-meta; surface that changes with viewing angle [13]

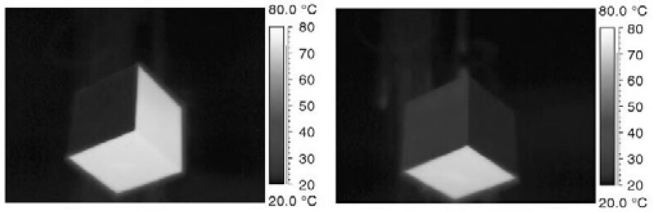

Fig. 6 A polished copper face cube vs. an unpolished copper face [13]

E. Thermal Reflection

The thermal radiance emitted by other bodies (atmosphere and/or other structures) also plays a role in thermography. From Fig. 7, it can be seen that the surface with the lower emissivity shows higher reflection of the external thermal radiance. This is due to what Kirchoff's law states, the polished surface does not emit as much thermal radiation of the surface and therefore, it does not absorb as much thermal radiation either. Thus, the thermal radiance emitted from other bodies does not become absorbed, but is rather reflected. The inverse can be seen for the painted surfaces where high emissivity, which is high emittance, has high absorption. Accordingly, external thermal radiance is absorbed.

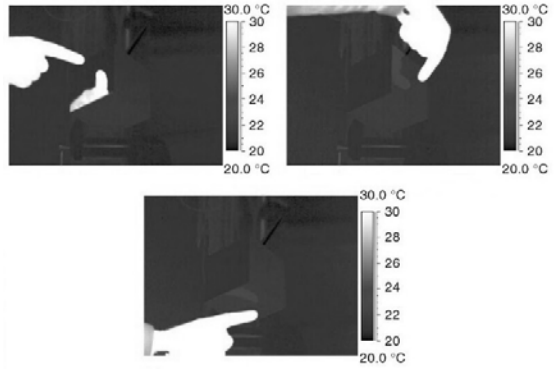

Fig. 7 A polished copper face vs. a white painted face vs. a black painted face [13]

F. Active and Passive Heating

Active thermography is actively heating the surface to produce a usable thermal gradient (the voids and continuous medium clearly show difference in temperature). This active heating is achieved by the use of halogen or infrared lamps and thus can become a costly activity. Passive thermography is when there is natural thermal radiation to produce a sufficient thermal gradient without the use of any external heating equipment. The advantages are naturally the cost of the usage of thermography but also in Southern Africa the natural heating of the sun throughout the year provides a widespread viable area for testing, unless the testing is to be done indoors where sun is not present. The disadvantages to the sun being the heat source is that the surface being tested is outside and so open to environmental fluctuations [3].

III. Experimental Design

A. Purpose of Experiment

This study will determine whether it would be viable to substitute the existing time-consuming diagnostic methods with that of using a RPAS system with a thermal camera attached. Using this equipment to easily maneuver the camera around the structures could decrease the time needed to do the testing and so reduces costs and possible safety risks involved. Finding the optimal method of capturing the images with the RPAS will be tested to verifying if the data captured can be compiled into a 3D-model to ease the presentation of the data to a client.

B. Experimental Setup

A concrete wall, 1.2 m x 1.1 m and 0.3 m thick, had embedded polystyrene shapes which were a circular defect with 300 mm diameter on the western side of the surface and a square defect, 300 mm x 300 mm on the eastern side of the surface. These embedments were 50 mm beneath the northern facing surface, of which the footage was captured. An I-beam was cast in the wall to stabilize the wall on the ground. The thermal camera used was a FLIR Tau thermal imaging camera core. The core was mounted onto the RPAS and wired to be able to toggle the capturing of the images manually. The setup was located at an overflow parking area on UJ APK campus to ensure little disturbance to the setup and keep the public away from the setup.

C. Methodology

Two sets of tests were taken at 12:00, 14:00 and 17:00. Each was done at a distance of four meters away from the concrete surface whilst moving in an arc around the wall. First set captured was with the camera levelled, having no vertical angle, at the same height as that of the defects. In the second set the camera was lowered by 500 mm and tilted upwards facing the defects. Specific measurements of temperature were taken for both sets at different viewing angles; at a perpendicular view (90°), 45° and near parallel to the surface (0°) to the surface. The collection of these temperatures was plotted to analyze the effect quantitatively of how the change in horizontal angle affected the temperature difference between the defects and the concrete wall for both sets of images. These readings were taken over a time period as to obtain the averages used to compile the results. The images that were captured continuously whilst moving in an arc were used to construct the 3D models.

IV. Results

A. Differential Temperatures on Specific Angles

For the 12:00 set of images, the temperature over the wall was measured on a fixed line moving over the defect position. The first set of data was captured where the camera had no vertical angle. These data are shown in Fig. 8, the left peak represents the temperature over the square defect and the right the temperature over the circular defect. The minimum value represents the temperature of the wall where no defects are present. The difference in temperature between the peaks and the trough is what will be visible on the images. It can be seen in Fig. 8 that as the viewing angle decreases the differential temperature decreases slightly, however at very acute angles this difference becomes much more visible. The size of the defects can be measured on the perpendicular images. The square was measured as 295 mm (41 pixels of the walls total breadth of 167 pixels) and the circular defect as 302 mm (42 pixels). The second set of data was captured where the camera had a slight vertical angle. It can be seen on Fig. 9 that with a decreasing horizontal viewing angle the temperature difference between the wall and the defects becomes much more apparent. This results in poorly visible defects on the images. The differential temperatures of the square and circular defect were found to be 4.3 °C and 3.2 °C respectively. These temperatures were calculated by negating the average temperature of the defects to that of the average temperature of the wall. From the data collected where there was no vertical angle, the average temperature of all the defects showed a maximum variance of 0.2 °C. The data showed that where there was a vertical angle present, the differential temperature of the square and circular defect was found to be 4.3 °C and 3.3 °C, respectively. The maximum variance however was found to be 1.3 °C, from the acute angles, much larger than that of the data where there was no vertical angle present.

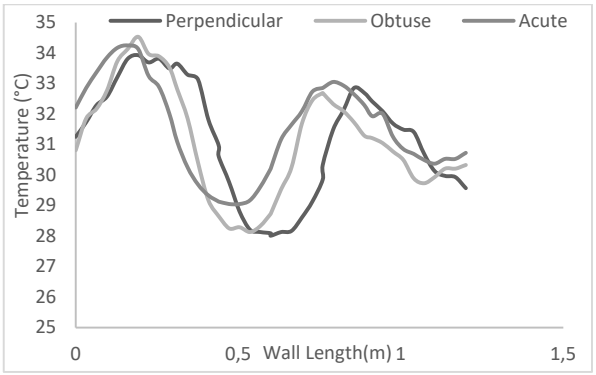

Fig. 8 Line temperature for 12H00 readings with no vertical angle tilt

B.3D Model Composition

Baseline reference model for normal photographs: For a reference a 3D model was made by using normal photographs. The same method was used to capture these images as with the thermal images. In the black and white figures, darker areas indicate higher temperatures. The baseline model can be seen in Figs. 10 (a) and (b), showing the Northern view and the North-Western view of the wall investigated for this research.

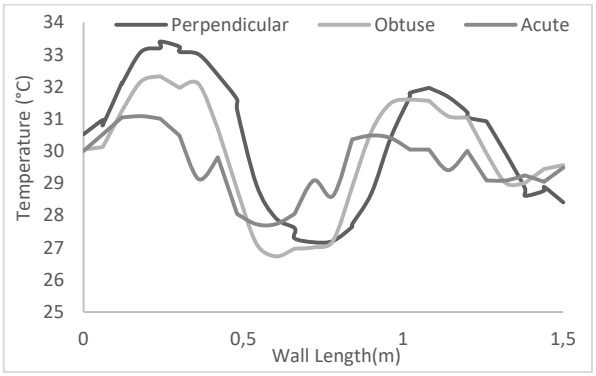

Fig. 9 Line temperature for 12H00 readings with vertical angle tilt

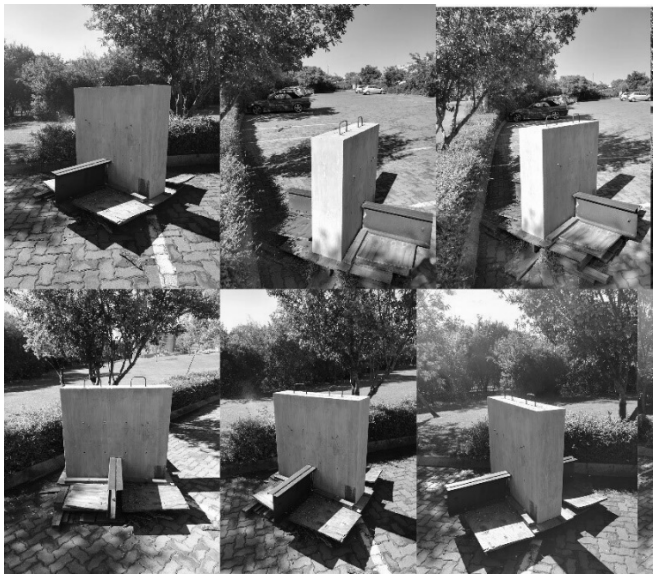

Fig. 10 (a) Baseline 3D Model

Fig. 10 (b) Northern and North-Western view of wall

12H00 3D thermal model: The images from 12:00 were compiled to create the model as shown in Figs. 11 (a) and (b). The defects are clearly visible. However, the surface produced is not a true representation of that of the physical surface, but the general shape and size can be seen. The square defect is seen on the left and the circular defect on the right.

14H00 3D thermal model: The images from 14:00 were compiled to create the model as shown in Figs. 12 (a) and (b). The surface is very distorted at the top side of the wall and the defects are barely visible on the model. The defects are however slightly visible on the images used to produce the model, showing that the defects must be clearly visible to show on the model.

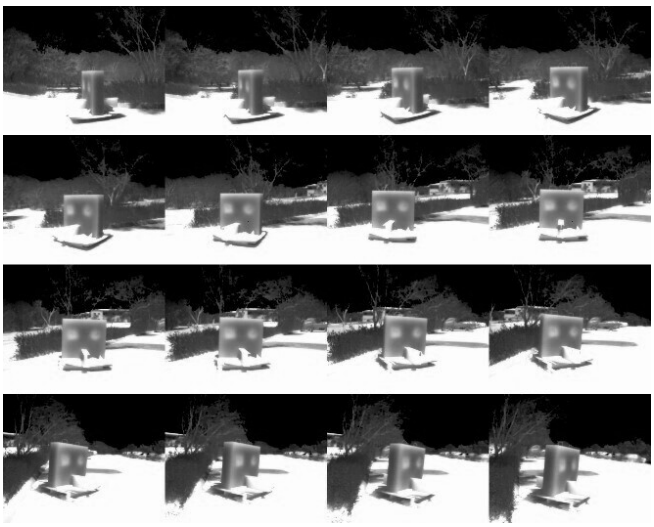

Fig. 11 (a) Thermal photos: 12H00

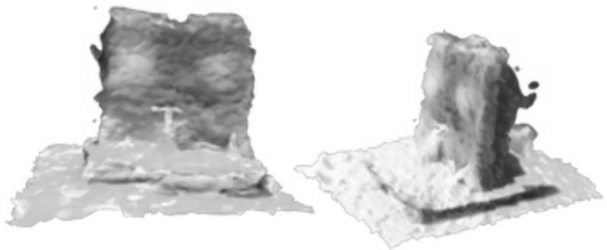

Fig. 11 (b) Thermal model: 12H00

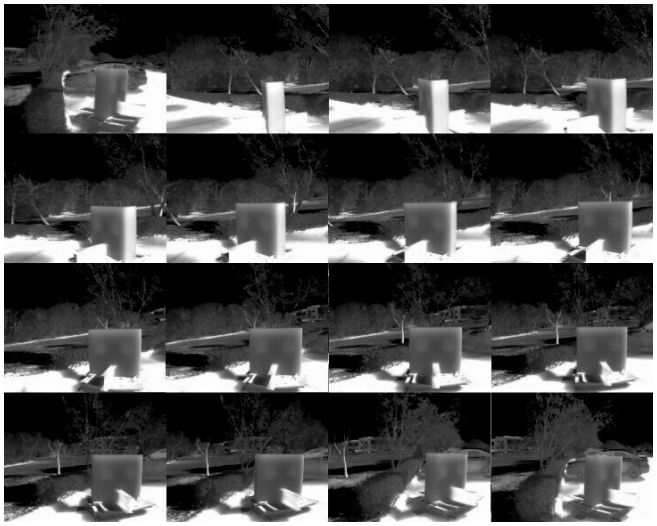

Fig. 12 (a) Thermal photographs: 14H00

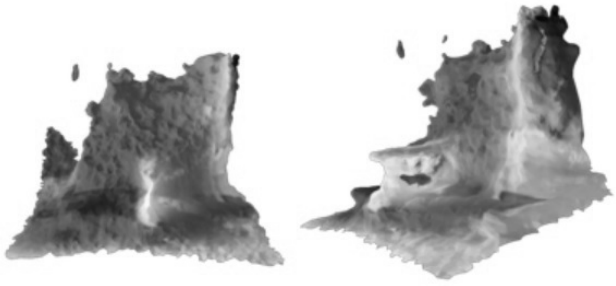

Fig. 12 (b) Thermal model: 14H00

17H00 3D thermal model: The images from 17:00 were compiled to create the model as shown in Figs. 13 (a) and (b). This model shows similar distortion to that of the 14:00 model, distorted and an irregular surface. The defects on the images used for the model were barely visible and so there is no trace of the defects in the model and can be seen from the results of the small differential temperature between the defects and the wall.

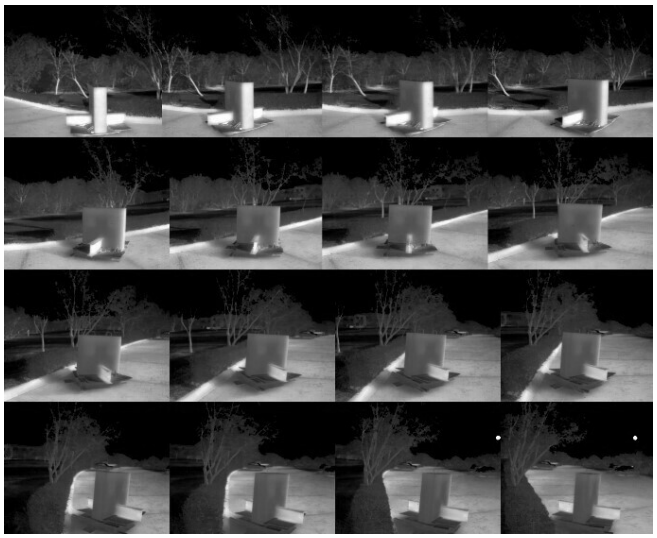

Fig. 13 (a) Thermal photographs: 17H00

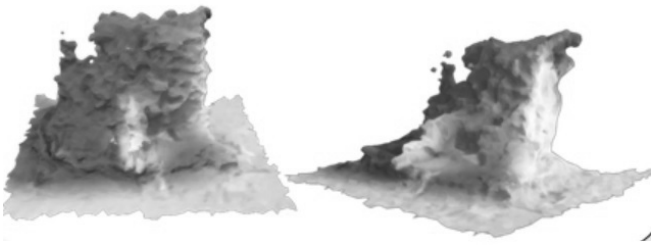

Fig. 13 (b) Thermal model: 17H00

V. Application of Thermography

Similar to the standard methods used by Washer [1], the ASTM standard testing methods for applying the technology for bridge decks show that a similar application can be used for high-rise concrete structures. This leads to the use of a RPAS with a thermal camera to be used to evaluate concrete surface at higher altitudes. The results show that the environmental conditions (time of day, weather conditions) and thermal gradient of the concrete is critical for adequate results. Therefore, guidelines on such an application must be composed to standardize such an application.

VI. Conclusion

The change in the horizontal angle shows minor changes in the differential temperature until the angle becomes too acute. This effect becomes more apparent when a vertical angle is introduced. As a result, it is recommended that any images taken must be done as perpendicular as possible to the surface being captured. The best images, showing the largest differential temperature between the defect and the concrete, were captured at 12:00 (when the sun is at its highest). The 12:00 model showed the best results where the defects are clearly visible, and the shape of the wall is recognizable. The surface irregularities might be due to the low resolution of the thermal camera together with the lack of "unique" features as seen in normal photographs that works well with photogrammetry. The use of an RPAS drastically reduces the risks and time to capture the thermal images. This leads to a great reduction in cost of the application as less manpower is used as well as less time to cover the concrete structure. However, it should be noted that legal aspects could increase the capital cost of the application as well as the limits of the application (flight height, distance from public, restricted airspace). The fees and regulations of the legislation of an RPAS must be assessed based on the country of usage. The legislation together with what is discussed above, about the environmental aspects of the viability of thermography, must be used to create guidelines and standards to which the application of thermography with an RPAS can be used.

References

[1] Washer, G., Fenwick, R. & Nelson, S., Guidelines for the hermographic Inspection of Concrete Bridge Components in Shaded Conditions. Columbia: University of Missouri, 2013.
[2] IAEA, Guidebook on non-destructive testing of concrete structures, International Atomic Energy Agency, Vienna, 2002.
[3] Scott, M. et al., Passive infrared thermography as a diagnostic tool in civil

engineering structural material health monitoring. Johannesburg: University of Johannesburg, 2012.
[4] van der Merwe, J.J., An Investigation into the Impact of the Viewing Angle of an elevated concrete structure diagnostics using. University of Johannesburg: University of Johannesburg, 2015
[5] P. van Tonder, "Infrared Thermography (IRT): Parameters effecting IRT and analysis of the IRT patterns," University of Johannesbrug, Johannesburg, 2016.
[6] ICRI, Award of Merit: Special Projects Category, Preservation of LSU Tiger Stadium. 2013, (Online) Available at: https://www.icri.org/page/AOM13_LSUTigerStadiu (Accessed 28 May 2018)
[7] Vorster, D.J. & Gräbe, P.J., 2013. The use of groundpenetrating radar to develop a track substructure characterisation model. *Journal of SAICE*, 55(3), p.715
[8] EENA, Remote Piloted Airborne Systems (RPAS) and the Emergency Services, RPAS and the Emergency Services. Brussels, 2015.
[9] Lewis, K., Drones for flood control infrastructure inspection in Denver. Denver, U.S, 2016.
[10] Department of Transport, Civil Aviation Act, 2009 (Act No. 13 of 2009). *Government Gazette*, 27 May 2015. Available at: http://www.caa.co.za/Legal%20Documents/PART%20101%20GAZETTE.pdf.
[11] ICRI, Award of Merit: Special Projects Category, Structural Reinforcement of Florencia Resort Complex Condominiums. 2010 (Online) Available at: https://www.icri.org/page/AOM10_FlorenciaResor (Accessed 28 May 2018).
[12] Vollmer M, Mollmann K, Fundamentals of Infrared Thermal Imaging, Chapter 1, Wiley, November 2017. 7–588, Apr. 1965.
[13] C. Kuenzer and S. W. Dech, Thermal Infrared Remote Sensing Sensors, Methods, Applications, Germany: Dordrecht: Springer, 2013.
[14] Mikron Instrument COmpany Inc., "Table of Emissivity of Various Surfaces," Transmetra, 2003.